Fifth International
Dam World Conference
PORTUGAL • LISBON • LNEC • APRIL 13-17, 2025

# STABILITY ANALYSIS OF CONCRETE DAM FOUNDATIONS FOLLOWING A HYBRID DISCRETE ELEMENT/FINITE ELEMENT APPROACH



**N. Monteiro Azevedo**[1]
LNEC

**M.L. Braga Farinha**
LNEC

**S. Oliveira**
LNEC

## ABSTRACT

In concrete dam foundations, failure mechanisms are primarily influenced by natural rock discontinuities, the dam-foundation interface, or weaker strata. Instability can manifest beneath the dam, within the abutments, or along adjacent slopes. For arch dam foundations, particular attention is required for failure scenarios involving sliding along weaker surfaces in areas where the arches are supported (along the valley sides and abutments), as well as issues related to seepage at the valley bottom, that may lead to the discontinuities erosion. Sophisticated analyses employ discrete element models, which capture well the discontinuous nature of rock and can incorporate fluid flow through these discontinuities. In stability analyses of concrete dam foundations, interface models whether based on discrete element or finite element techniques typically use planar joint formulations, such as point-to-point, point-to-surface, and edge-to-edge contacts. This paper introduces a new hybrid discrete element/finite element approach. When large displacement may occur, the rock blocks outer surfaces are discretized with spherical particles, allowing interactions to be modelled through particle-to-triangular surface interactions which are known to be computationally robust. Whenever possible, the contact interaction is defined in small displacements using finite element joint elements. A simplified gravity dam equilibrium example is presented to validate the proposed hybrid model. Stability analysis of an idealized arch dam foundation is also performed. The presented results are shown to closely match those obtained with a more complex polyhedral-based discrete element model.

**Keywords:** concrete dams, rock foundations, stability analysis, contact interaction, hybrid model.

[1]nazevedo@lnec.pt, Portugal

## 1. INTRODUCTION

The foundation rock mass of concrete dams is a crucial element in the safety of this type of construction, as most failures occur due to problems in the foundation. The behavior of the rock mass is influenced by the load transfer mechanism from the dam body to the foundation. In concrete dams, failure mechanisms usually involve discontinuities in the foundation rock mass, the dam/foundation contact surface or layers of rock mass with lower resistance. Instability can occur under the dam, at the abutments or on the adjacent slopes.

In the case of arch dam foundations, special consideration must be given to failure scenarios involving sliding along surfaces of lower strength located in the arch support zone, particularly at abutments and mid-slope areas, and those involving percolation in the valley bottom zone, which leads to the erosion of discontinuities [1, 2]. The safety of this type of structures requires the use of three-dimensional models and the consideration of water pressures in the foundation discontinuities [3].

Stability assessments have been carried out in recent years using three-dimensional discrete element models, in which the blocks of the rock mass are represented by deformable polyhedral blocks, discretized with an internal mesh of uniformly stressed tetrahedral finite elements. Simplified pressure fields are usually assumed, determined considering the water level in the reservoir, the existence of the drainage curtain, and a phreatic surface downstream of the work compatible with the slope inclination. In [1] these pressures are obtained by performing hydraulic calculations with equivalent continuous medium models and in [3, 4] a 3D discontinuum hydromechanical model is used that performs a fully coupled hydromechanical analysis, where fracture conductivity is dependent on mechanical deformation.

This paper proposes a new hybrid discrete element/finite element approach. When large displacement may occur, the rock blocks outer surfaces are discretized with spherical particles, allowing interactions to be modelled through particle-to-triangular surface interactions which are known to be computationally robust. For this purpose, the interior domain of each block is discretized with spherical particles that interact with the triangular surfaces adopted in the discretization of the neighboring blocks. In [5] a similar algorithm for interaction between deformable blocks is proposed, in which the contact surfaces of each block are approximated by spherical particles. Whenever possible, the contact interaction is defined in small displacements using finite element joint elements. A similar contact rounding scheme that adopts inscribed spheres at the block vertexes and inscribed cylinders at the block edges has been proposed for contact recognition in discontinuous deformation analysis (DDA) [6, 7].

The 3D large displacement contact scheme is based on the 2D circular particle/side interaction model proposed in [8, 9]. In [10] it is also proposed a particle-particle interaction model for particle systems, which defines the unit normal of the contact as a function of the joint plane to which the contact belongs, thus reducing the influence of the roughness of the particle-particle contact. This particle-particle interaction algorithm has been applied to 3D slope stability analysis [11].

The proposed approach for large displacement interaction that adopts spherical particle/spherical particle or spherical particle/triangular surface interactions is not only simpler but also more computationally robust than models based on the actual geometry of each block [7, 8].

A simplified gravity dam equilibrium example is presented to validate the proposed hybrid model and to highlight the relevance of adopting a large displacement contact model when evaluating the associated safety factor. The stability analysis of an idealized arch dam foundation is also performed, the presented results are shown to closely match those obtained with a more complex polyhedral-based discrete element model.

## 2. 3D HYBRID DISCRETE ELEMENT/FINITE ELEMENT MODELLING

### 2.1. General formulation

The mechanical model adopted is a discrete model that uses an explicit solution algorithm based on the central difference method [14]. Each block of the model is internally discretized with a mesh of tetrahedral or 2nd degree hexahedral finite elements, to take its deformability into account. Figure 1 shows the calculation cycle of the explicit mechanical model adopted.

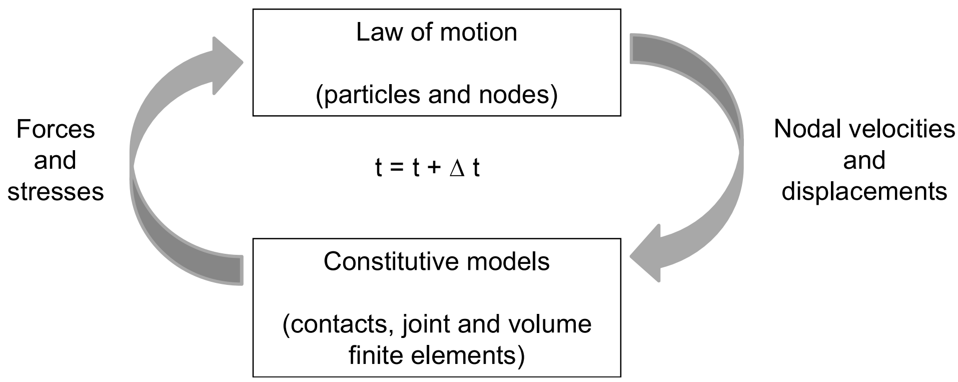


**Fig. 1 – Mechanical model calculation cycle**

For a given nodal point or spherical particle, the equations of motion are given by:

$$\mathrm{m}\ \ddot{u}_i(\mathrm{t}) + \mathrm{c}\ \dot{u}_i(\mathrm{t}) = F_i(t) + m\ g_i \tag{1}$$

where $\dot{u}_i$(t) is the velocity, $\ddot{u}_i$(t) is the acceleration, $c$ is the damping constant, $m$ is the nodal mass, $g_i$ is the acceleration due to gravity and $F_i(t)$ are the nodal forces acting at a given instant defined by three terms:

$$F_i(t)=F_i^e(t)+F_i^c(t)+F_i^l(t) \tag{2}$$

where $F_i^e(t)$ are the external forces applied at the nodal point, $F_i^c(t)$ are the external forces due to contact with neighboring blocks that only exist at the nodal points on the block boundary, and $F_i^l(t)$ are the internal forces due to the deformation of the associated plane finite elements. Equation 1 is integrated using the central difference method, which is conditionally stable. The definition of the calculation step and the solution scheme to be adopted when only the static solution of the problem is required can be found in [14].

The interaction between deformable blocks can be carried out using discrete element techniques, which make it possible to analyze large displacements. In 3D there are 6 different types of contact, defined according to the elements used to represent the surface of the block: vertices (V), edges (A) and faces (F). There are two fundamental types of interaction that need to be modelled and which allow the correct definition of the various types of contact: vertex-face interaction (VF) and edge-edge interaction (AA) [15].

Joint finite elements [16, 17] require the finite element meshes of each block to be compatible, and are generally suitable for analysis at small displacements. This type of formulation has the advantage of allowing perfect compatibility of the displacement field along the interfaces between elements of the same degree. Thus, for similar discretizations, a more accurate representation of the stress distribution along the interfaces is obtained than with traditional discrete element models. However, this formulation requires more robust generation schemes to ensure that the interactions in 3D are only of the face/face type [3], or in 2D of the edge/edge type [8].

## 2.2. Large displacement contact model

### Spherical particle/triangular surface interface model

The spherical particle/triangular surface interface model between deformable blocks is based on the particle/wall contact model traditionally adopted for contact between rigid elements [14]. The interface model considers the deformability of each block, since it considers the influence of the mesh, tetrahedral finite elements or hexahedral finite elements adopted in the discretization of each block, in the definition of the relative contact velocity and the distribution of the contact force.

Thus, as in the rigid model, the contact between the spherical particle belonging to a given block and the triangular surface of the neighboring block presents, at each instant, a normal given as a function of the area of the triangular surface that interacts with the spherical particle (Figure 2a). The overlap between the spherical particle and the triangular surface at the point of contact and the location of the point of contact is given by:

$$U^n = R^{[B]} - d \tag{3}$$

$$x_i^{[c]} = x_i^{[B]} + (R^{[B]} - \tfrac{1}{2} U^n)\, n_i \tag{4}$$

The contact point velocity is given by the relative velocity of each entity at the contact point, thus:

$$\dot{x}_i^{[c]} = \dot{x}_i^{[ST.C]} - \dot{x}_i^{[B.C]} \tag{5}$$

where the velocity of the triangular surface $\dot{x}_i^{[ST.C]}$ and the velocity of the particle $\dot{x}_i^{[B.C]}$ are defined as a function of the value of the shape functions at the contact point of the tetrahedral element or hexahedral element associated with each entity, and their nodal velocities. For the case of a spherical particle (*B*) associated with a tetrahedron of nodes *i,j,k,l* (Figure 2 b), the velocity at the point of contact is given by:

$$\dot{x}_i^{[B.C]} = N^i \dot{x}_i^i + N^j \dot{x}_i^j + N^k \dot{x}_i^k + N^l \dot{x}_i^l \tag{6}$$

For a given tetrahedron the shape function associated with node $^i$ is defined as a function of the volumes of the following tetrahedrons:

$$N^i = \frac{Vol\,\Delta\,(j.l.k.x^{[c]})}{Vol\,\Delta\,(i.j.k.l)} \tag{7}$$

The proposed model assumes that the spherical particles used in the internal discretization of each block are rigidly connected to the finite element (*s*) that intersect their center of gravity. The shape functions associated with each spherical particle are therefore defined at the start of the calculation, and these shape function values are constant throughout the simulation. These values are used to define the new positions of the spherical particles needed to define the contact point.

The displacement increment of each local contact point, associated with the interval $\Delta\, t$ in the normal, $\Delta\, x_n^{[c]}$, and shear components, $\Delta\, x_{s,i}^{[c]}$, is determined using the following expressions:

$$\Delta\, x_n^{[c]} = (\dot{x}_i^{[c]} \Delta\, t) n_i \tag{8}$$

$$\Delta\, x_{s,i}^{[c]} = \dot{x}_i^{[c]} \Delta\, t - \Delta\, x_n^{[c]}\, n_i \tag{9}$$

In the adopted formulation, the normal component of the displacement of the local contact point corresponds to a scalar quantity and the tangential component corresponds to a vector quantity. The increments of normal force, $\Delta\, F_n^{[c]}$, and shear force, $\Delta\, F_{s,i}^{[c]}$, at each local contact point are determined according to a linear force-displacement relationship as a function of the normal stiffness, $k_n$, and shear stiffness, $k_s$, associated with the local contact and the relative displacement:

$$\Delta F_n^{[c]} = -k_n \, \Delta x_n^{[c]} \tag{10}$$

$$\Delta F_{s,i}^{[c]} = -k_s \, \Delta x_{s,i}^{[c]} \tag{11}$$

It should be noted that the normal and shear stiffnesses are defined as a function of the particle's diameter. At a given moment, the resultant force at the point of contact is given by the sum of the normal component and the shear component using the following expression:

$$F_i^{[c]} = F_n^{[c]} n_i + F_{s.i}^{[c]} \tag{12}$$

The contact force is transferred to the nodal points of the finite element associated with the spherical particle and to the nodal points of the finite element associated with the triangular surface. Thus, for the nodal point *i* of the tetrahedron *ijkl* associated with the particle *B*, the internal force of the nodal point is updated given the value of the shape function associated with the nodal point to:

$$F_i^{[i]} = F_i^{[i]} - F_i^{[c]} N^i \tag{13}$$

For the nodal point *m* of the *mnop* tetrahedron associated with the triangular surface, the internal force of the nodal point is updated given the value of the shape function associated with the nodal point using the following expression:

$$F_i^{[m]} = F_i^{[m]} + F_i^{[c]} N^m \tag{14}$$

The mass scaling technique can be adopted if only a static solution is required [14] that increases the algorithm's convergence rate by reducing the ratio between the system's minimum and maximum frequencies. In this case, the mass of each nodal point is changed at each calculation step to guarantee the stability of the algorithm for a unit time increment. The normalized mass is determined using the following expression:

$$m_{escalada} = 0.25 \, K_t \tag{15}$$

The translation stiffness, $K_t$, of each nodal point must consider the contribution of all contacts and all associated finite elements. An upper limit on the contribution of a given contact to nodal point i, not considering the orientation of the contact plane, is given by:

$$K_t = \sum_{c=1}^{N} 2 \, (k_n + k_s) \tag{16}$$

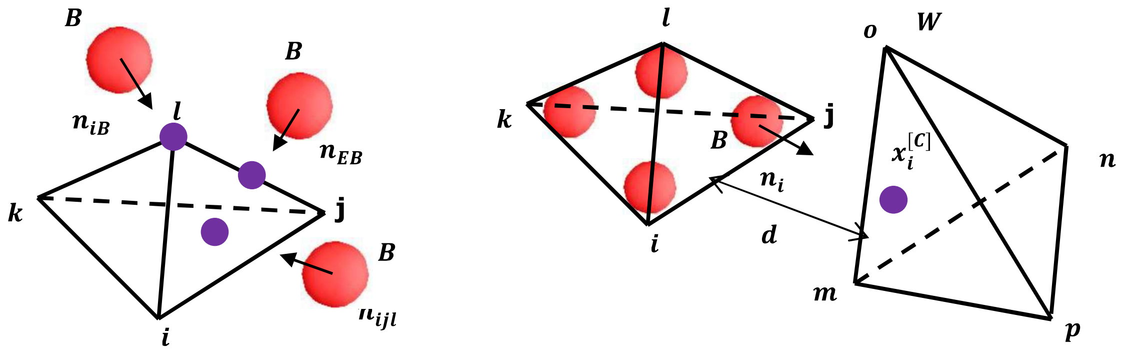


$n_{EB}$ *Zone* 1: *Edge normal*

$n_{iB}$ *Zone* 2: *Vertex normal*

**a) Contact normal direction depends on the location of the particle/block contact point**

b) **Geometry of the contact between a particle (*B*) inside a block and the outer triangular *mno* surface (*W*) of another block**

**Fig. 2 – Point contact spherical particle (*B*)/triangular surface (*W*)**

### Internal discretization of a given block

In the proposed contact model, it is necessary to previously discretize each block with a particle system, adopting the models proposed in [14]. After defining a compact particle system, the interior particles that are not in contact with the block exterior surfaces are discarded. Finally, the particles, which come to represent the outer geometry of the block, are classified according to their position, as shown in Figure 3. The radius of the particles representing the outer geometry of the block are then redefined to bring the sum of the areas associated with the spherical particles as close as possible to the area corresponding to the outer surface they represent. The contact stiffness values are determined considering these new particle radius values.

It is necessary to classify the particles according to their positioning, as the unit normal of the contact must be corrected to ensure that the roughness of the outer surface of the particle system does not influence the interaction between blocks, avoiding the appearance of artificial entanglements. Figure 4 shows the corrective measures to be adopted when redefining the contact normal depending on the classification of the particle and the positioning of the contact on the triangular surface.

With this approach, the level of discretization of the contact is independent of the internal finite element mesh used to represent the deformability of the block and is given as a function of the particle size used in the discretization of each block.

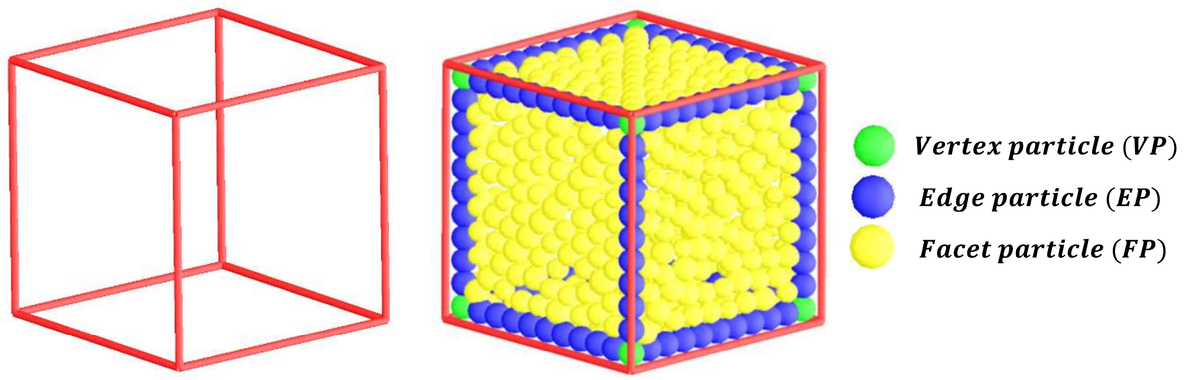


**a) Block without particles** **b) Block with the classification of particles that represent the exterior surface**

**Fig. 3 – Internal discretization of a block by a system of particles**

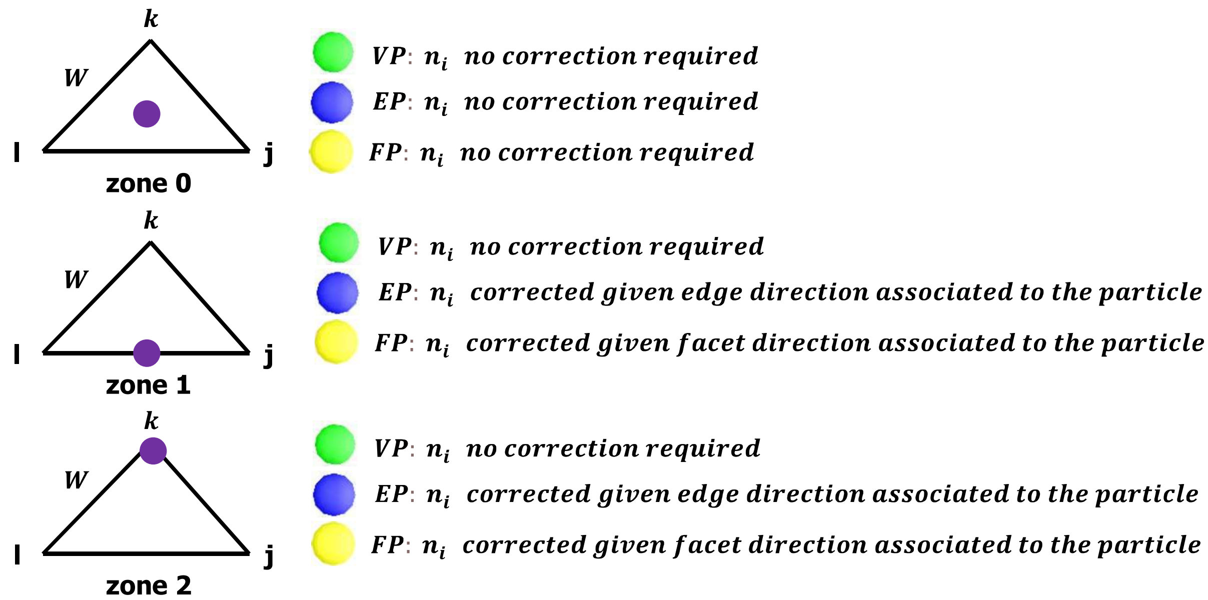


**Fig. 3 – Correction of the unit normal of the contact depending on the location of the contact in relation to the triangular surface (*W*) and the classification of the spherical particle**

With this approach, the level of discretization of the contact is independent of the internal finite element mesh used to represent the deformability of the block and is given as a function of the particle size used in the discretization of each block.

## 3. CASE STUDIES

### 3.1. Gravity dam stability analysis

The stability of a 30 m high gravity dam is assessed. The geometry of the gravity dam model is shown in Figure 5. As shown, several discontinuities were considered in the rock foundation. Three numerical modes were developed. In the first model the block interaction was carried out using only interface joint elements suitable for small displacements, FE-SD, in the second model an internal discretization with particles with 0.50 m radius in the areas where large displacements are expected to occur was adopted, PM-LD, and in the third model an internal discretization with particles with 0.50 m radius in the areas where large displacements are expected to occur was adopted, but the interaction between the fracture media and the foundation base is carried out using joint finite elements, Hybrid-FE&PM.

In all developed models, 8 node hexahedra elements are adopted in the volume discretization, 57 finite elements are adopted in the dam, 84 finite elements are adopted in the fracture media and 288 finite elements are adopted in the base, Figure 6a). In the FE-SD model joint finite elements are adopted for block interaction purposes, 57 joint elements represent the dam/fracture media interface, 84 joint elements represent the fracture media/fracture media interfaces and 96 joint elements represent the fracture media/base interface, Figure 6b). In the PM-LD a total of 6625 particles are adopted in the inner discretization of the outer boundary of the blocks that belong to the fractured media, Figure 6c). In the PM-LD the block interaction is represented by 2699 spherical particle/triangular surface contacts. In the Hybrid-FE&PM given that the interaction of the fracture media with the foundation base is carried out using joint finite elements only 1856 spherical particle/triangular surface contacts are required.

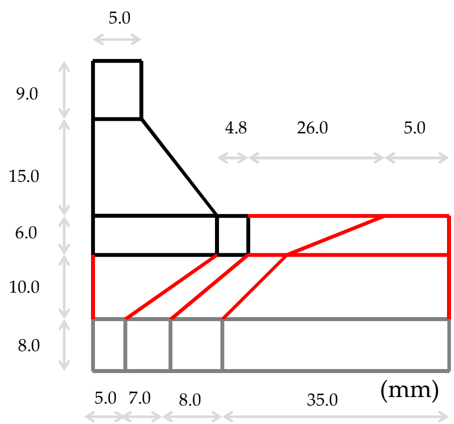


**Fig. 4 – Gravity dam geometry**

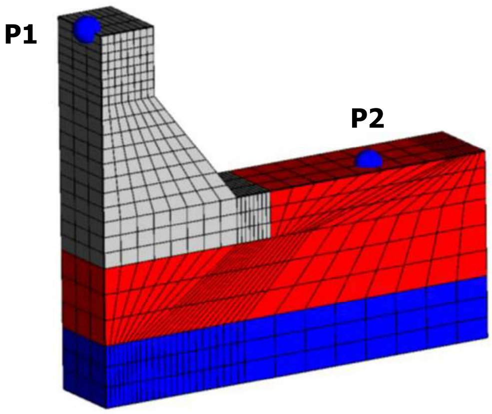


**a) 8 node Hexahedra finite elements**

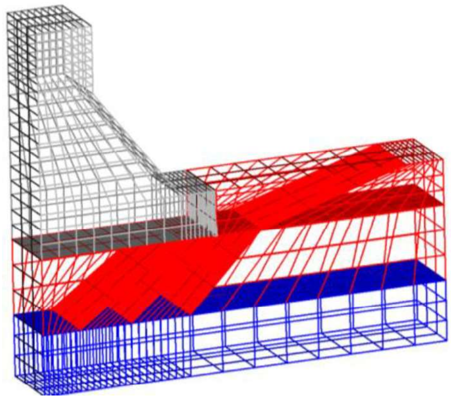

**b) 4 node Joint finite elements**

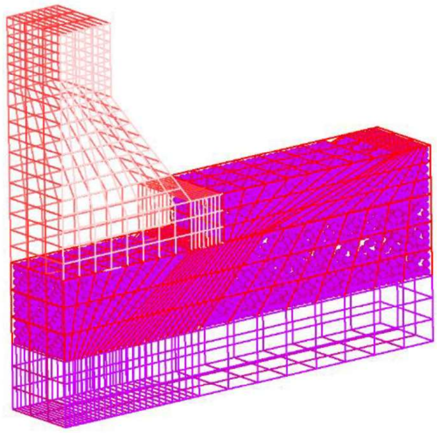

**c) Fracture media discretized with spherical particles for interaction purposes**

**Fig. 5 – Gravity dam numerical modes**

The mechanical properties adopted for the concrete and the rock foundation, and the elastic properties adopted for the contacts are presented in Table 3. The analysis was carried out in two phases, first the dam and rock mass weight were considered along with the hydrostatic pressure applied to the upstream section, assuming the level of the reservoir of 30.0 m. In this initial phase, linear elastic behaviour was considered in all interfaces. The calculations assumed that at the foundation base, zero displacement field is imposed in all directions. Following, a stability analysis was carried out by increasing the water pressure at the upstream face of the dam with an amplification factor ($\lambda$). In each cycle an increment in $\lambda$ equal to 0.2 was adopted. In the stability analysis all interfaces had a zero cohesion and tensile strength and a friction angle of 35.0º.

**Table 1 – Mechanical properties**

a) Volume FE elements

| Material | G (GPa) | v (-) | ρ (kg/m$^3$) |
|---|---|---|---|
| Dam concrete | 20.0 | 0.20 | 2.4 |
| Rock mass | 20.0 | 0.20 | 2.75 |

b) Joint FE elements

| Interface | $k_n$ (GPa/m) | $k_s$ (GPa/m) |
|---|---|---|
| Concrete/Concrete | 20.0 | 10.0 |
| Concrete/Rock | 20.0 | 10.0 |
| Rock/Rock | 20.0 | 10.0 |

Figure 7 shows the variation of the displacement in the upstream/downstream direction of points P1 and P2, see Figure 6a), with the hydrostatic amplification factor up to failure. As shown, a large displacement formulation predicts the initiation of a change in behaviour for lower amplification factors, whereas a small displacement formulation predicts less pronounced displacement variations up to failure. Figure 7 also shows that the response predicted with a Hybrid-FE&PM-LD is very similar to the response predicted with the model PM-LD that demands higher computational costs.

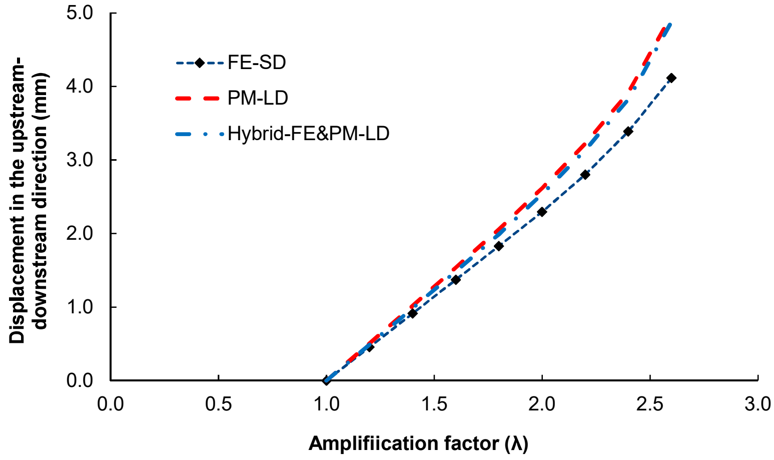


**a) Point P1**

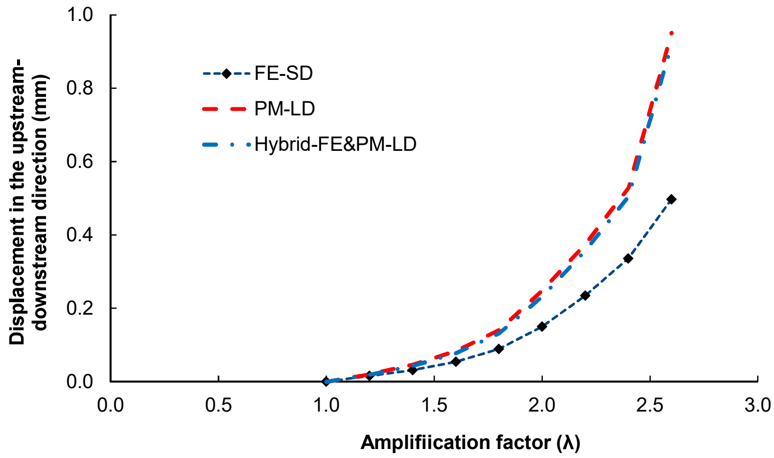


**b) Point P2**

**Fig. 6 – Variation of the displacement in the upstream/downstream direction with the amplification factor - Points P1 and P2 (see Figure 6a))**

Figure 8 presents the predicted failure modes for the FE-SD and the PM-LD models, as shown the predicted failure modes are similar, but at the onset of failure the FE-SD model based on small displacements does not guarantee that the correct final failure mode is obtained, whereas with a large displacement model, it is always assured that the failure mechanism is mechanically acceptable.

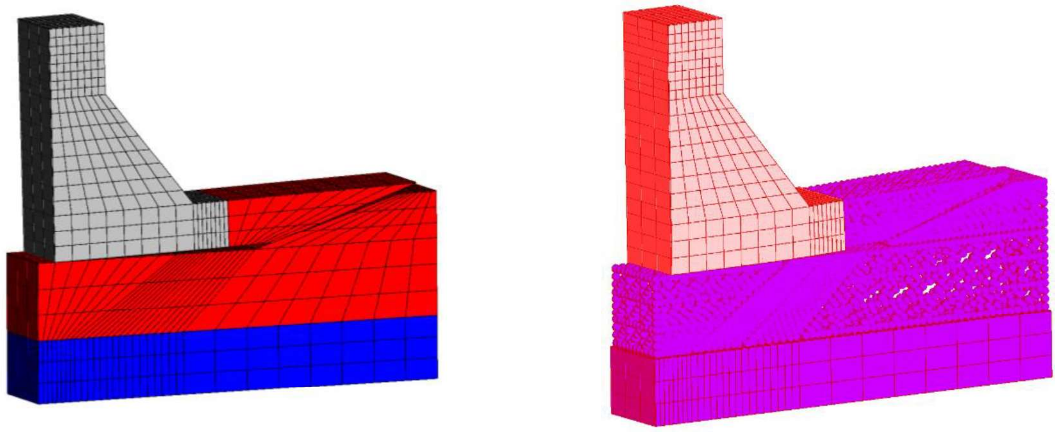

a) FE-SD b) PM-LD

**Fig. 7 – Failure modes**

## 3.2. Arch dam stability analysis

In this section stability of a hypothetical foundation of an arch dam is assessed. The geometric characteristics of the Talvacchia dam, located in Italy, were considered. The dam has a maximum height above the foundation of 77.0 m and the crown development is around 225.8 m. In the dam model shown in Figure 9, five dam contraction joints, the dam's insertion surface in the foundation, and two discontinuities in the foundation that define a hypothetical wedge in the rock mass on the right bank side, which provide a foundation failure mechanism. The three-dimensional finite element mesh used to represent the arch dam has two hexahedral 20 nodes finite elements on its thickness. Elements of the 1$^{st}$ degree tetrahedron type are used to discretize the foundation. The foundation model was generated in the 3DEC program [18].

With the proposed hybrid model two analyses were carried out: Hybrid-FE&PM (R=0.375), that adopts an internal discretization with particles with 0.375 m radius in the areas where large displacements are expected to occur, and Hybrid-FE&PM (R=0.75) which adopts an internal discretization with particles with 0.75 m in the areas where large displacements are expected to occur. Whenever possible, triangular joint elements were used in both models at the rock/rock and concrete/rock interfaces to reduce computational costs, in the other interfaces it adopts an internal discretization with particles at the vertices of the blocks. It should be noted that the 3DEC program's generation system does not guarantee perfect compatibility between the faces of the blocks, otherwise the analysis with the hybrid model could have been carried out using only triangular joint elements.

In the Hybrid-FE&PM (R=0.375) model all the blocks in the wedge zone are discretized with spherical particles with a 0.375 radius, Figure 10. A total of 75,509 particles are used in this zone. In the remaining zones, around 6493 spherical particles are used at the vertices of each block. In the Hybrid-FE&PM (R=0.375) model, around 4542 triangular joint elements and 66

2nd degree quadrangular joint elements (concrete/concrete interface) are adopted. In this model, around 61034 points of spherical particle/triangular surface contact are identified in the initial phase of the simulation. Figure 10 presents the interaction models, joint interface elements and triangular surfaces, adopted in the Hybrid-FE&PM (R=0.375) model.

In the Hybrid-FE&PM (R=0.75) model all the blocks in the wedge zone are discretized with spherical particles with a 0.75 radius. A total of 15755 particles are used in this zone. In this model, around 21274 points of spherical particle/triangular surface contact are identified in the initial phase of the simulation.

An analysis was also carried out using the 3DEC program with a similar mechanical model, in which the interactions between blocks follow the principles usually adopted in the interaction between polyhedral elements, considering the real geometry of the blocks. The model consists of 339 blocks (6 of which are the dam) with 9738 nodal points and the interaction between blocks is represented through 4441 contact points. The average size of the tetrahedral finite elements in the foundation is 25 m, except for the block at the base of the model where an average size of 40 m was adopted. The finite volume elements, 1st order tetrahedra and 20 node hexahedra elements, and the nodal points used to discretize the blocks are identical in the three models (Hybrid-FE&PM (R=0.375), Hybrid-FE&PM (R=0.750) and 3DEC).

The mechanical properties adopted for the concrete and the foundation rock mass and the elastic properties adopted for the contacts are similar to the previous example, Table 3. The same calculation procedure was followed for the three mechanical models adopted. The analysis was carried out in two phases, first the initial stress installed in the rock mass without the presence of the dam is considered, following the mechanical effect of the weight of the dam considering a model of independent cantilevers in the body of the dam is considered and finally the hydrostatic pressure to the upstream section is applied, assuming the level of the reservoir 5.0 m below the top of the dam. In this initial phase, linear elastic behaviour was considered in the various existing contacts. The calculations assumed that the rock mass has the following mechanical boundary conditions: zero displacement normal to the outer surface at the lateral boundaries and zero displacement in all directions at the outer surface corresponding to the base of the model.

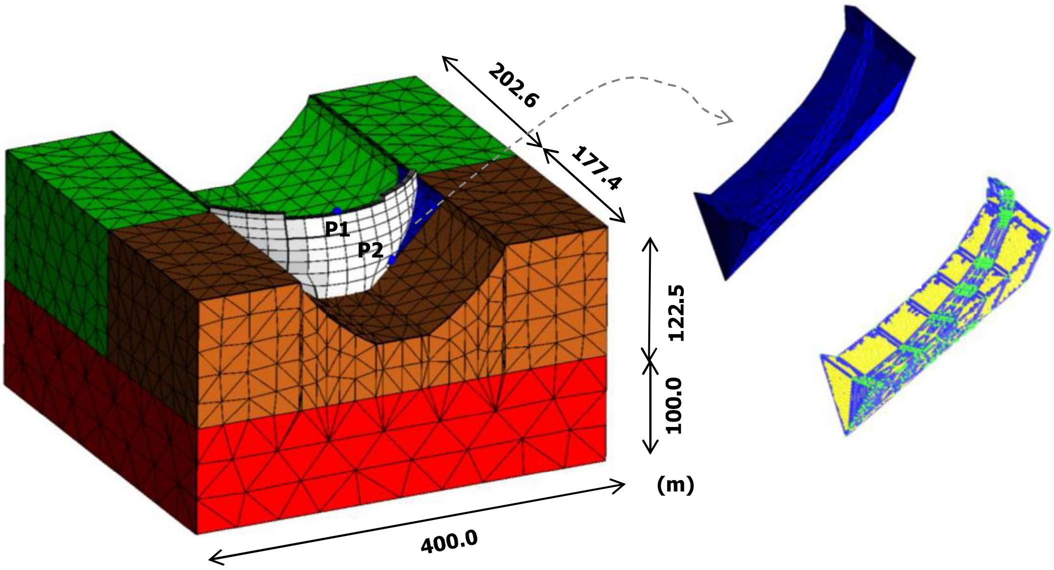


**Fig. 8 – Numerical model of the Talvacchia Dam including the rock mass and the internal discretization by a particle system of the zone where large displacements are expected to occur**

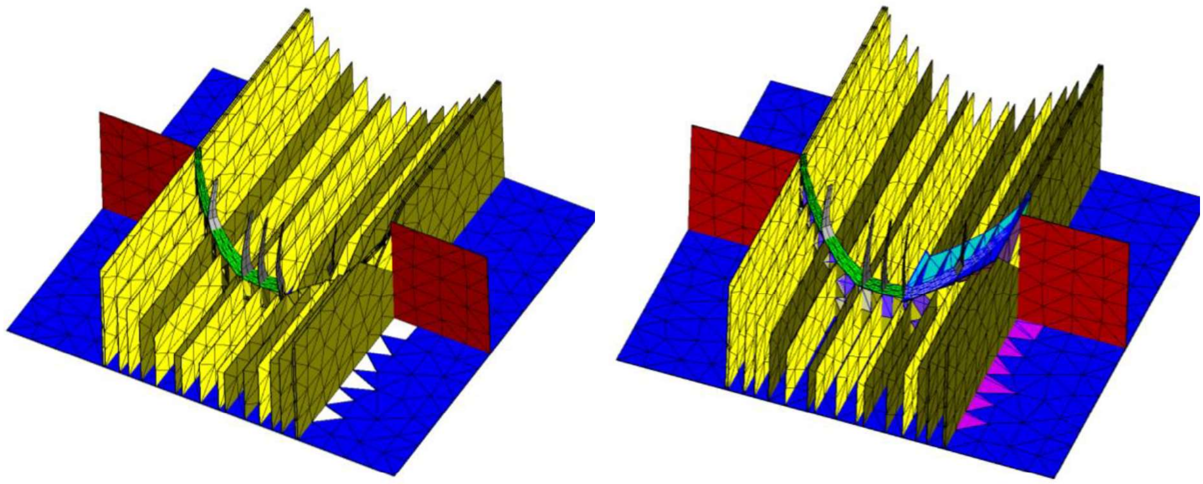

**a) Triangular joint elements and 2nd degree quadrangular joint elements**

**b) Interactions between blocks including spherical particle/triangular surface contacts**

**Fig. 9 – Interaction models - Hybrid-FE&PM (R=0.375)**

The stability analysis was carried out using the strength reduction method typically used in foundation design. The calculation process in the three models was similar. An initial friction angle of 35° was assumed in the discontinuities of the rock mass in the volume of influence of the wedge, with zero cohesion and tensile stress. A linear elastic contact model was adopted for the concrete/rock, concrete/concrete and other rock/rock joints outside the wedge's zone of influence.

In the stability analysis, a local damping model with a value of 0.70 was adopted for all the models [14]. The effect of water pressure on the discontinuities in the rock mass was not considered in the calculations, nor was the hydromechanical behaviour of the foundation rock mass. Figure 11 shows the displacement in the upstream/downstream direction evolution with the reduction in the friction angle in the discontinuities associated with the failure mode analyzed, Figure 10.

There is reasonable agreement between the proposed hybrid models and the 3DEC model. It can also be seen that for a value of zero friction angle, all models predict stable behaviour. The results presented in Figure 11 also show the relevance of adopting a higher outer boundary discretization, Hybrid-FE&PM (R=0.375), for which a more stable equilibrium configuration with lower displacements was predicted for a zero friction angle.

It should be noted that although the hybrid models and the 3DEC model reach a stable equilibrium configuration for a for zero friction angle values, the displacements recorded are already quite significant and the behaviour of the dam body is already quite far removed from that obtained for static initial loads. For this equilibrium position, the displacements both in the dam body and in the concrete/rock mass interfaces are already quite significant, and this position cannot be considered acceptable from a safety point of view. For friction angle values below 22º there is a clear change in the dam-foundation system behaviour, Figure 11, and the predicted displacements may compromise the dam safety.

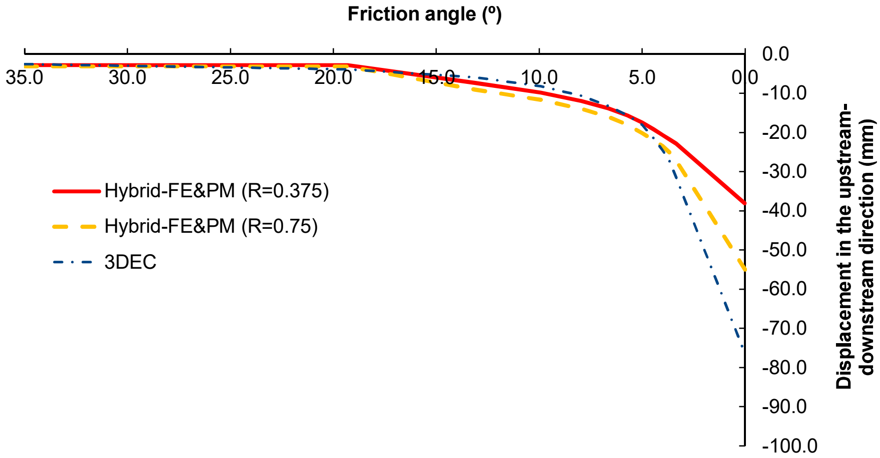


**a) Point P1**

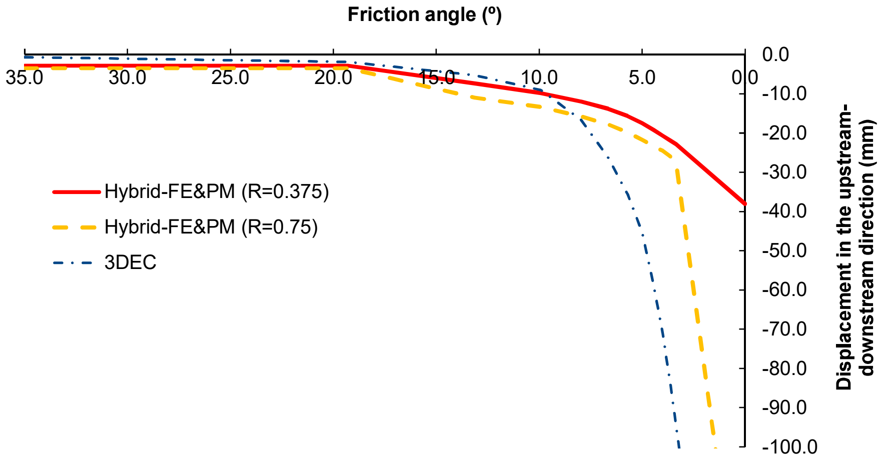


**b) Point P2**

**Fig. 10 – Displacement variation in the upstream/downstream direction with the reduction of the friction angle in the discontinuities associated with analysed failure mode - Points P1 and P2 (see Figure 10)**

Figure 12 shows the final deformation of the model obtained for a zero friction angle with a magnification factor of 10. A similar displacement field is obtained with the 3DEC model. Some of the independent blocks in the wedge zone show significant displacements and that, especially on the right bank, the support of the dam body on the rock mass is compromised, which is only possible because a linear elastic behaviour was considered in the vertical joints of the dam body.

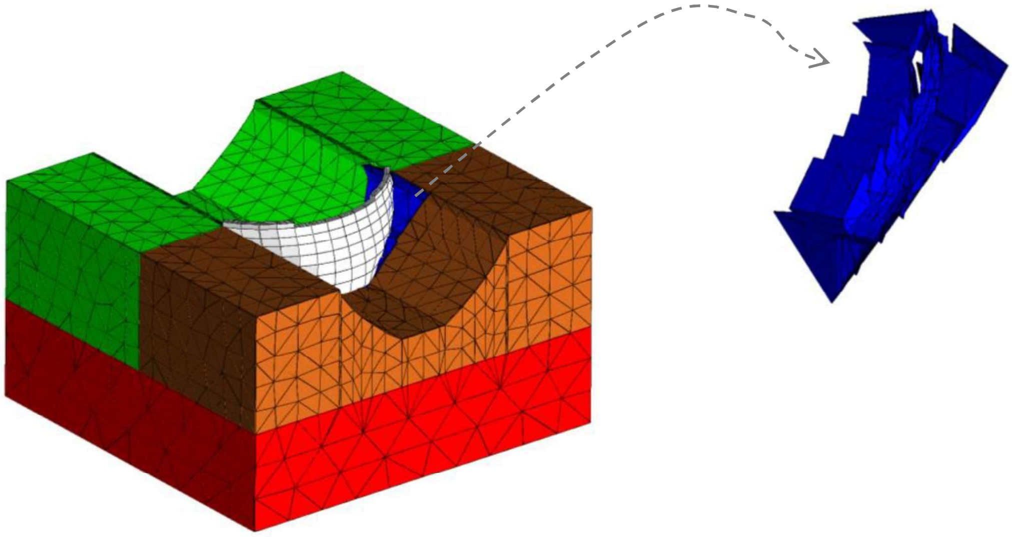

**Fig. 11 – Final deformation - 10x amplified displacement - Hybrid-FE&PM (R=0.375).**

## 4. CONCLUSIONS

This paper presents a new hybrid discrete element/finite element approach. Under large displacements, an interaction algorithm between neighbouring deformable blocks of the spherical particle/triangular surface type is adopted. The interior domain of each block is discretized with spherical particles that interact with the triangular surfaces adopted in the discretization of the neighbouring blocks, minimizing the effect of possible artificial entanglements.

The contact interaction scheme proposed for large displacement leads to an increase in computational requirements compared to other calculation schemes that consider the actual geometry of the block surface, as it requires the consideration of a greater number of contacts. However, the treatment of each contact is simpler, particularly when it comes to defining: i) the area of influence of each contact (particle diameter); ii) the normal of each contact (normal to the triangular facet); iii) the transition from a vertex/vertex contact to a vertex/face or vertex/edge contact and iv) the transition from an edge/edge contact to an edge/face contact. In order to reduce the associated computational costs, whenever possible, the contact interaction is defined in small displacements using finite element joint elements.

The proposed large displacement interaction scheme leads to a significant increase in the number of contacts, but it is a simpler and more computationally robust model than other schemes that take into account the actual geometry of the surface of the blocks. It should also be noted that with this approach the level of contact discretization is independent of the internal finite element mesh used to represent the block's deformability, and is given as a function of the particle size to be used in the discretization of each block.

The gravity dam shows that the proposed hybrid algorithm predicts a response closer to the response obtained with a full interaction model in large displacements. Note that a large displacement contact model is essential to obtain the correct failure mode. The presented arch dam foundation example shows that the proposed hybrid model for contact interaction predicts a response close to that obtained with discrete polyhedral elements based on more complex interaction models.

## ACKNOWLEDGMENTS

The study presented here is part of the research project StepDam: A step forward for the ability to anticipate and prevent failures of concrete dam foundations (Proc. 0403/1102/24145, included in LNEC´s Research and Innovation Plan 2021-2027. The authors express their gratitude to the Portuguese Foundation for Science and Technology (FCT) for funding the research project Seismic Monitoring and Structural Health of Large Concrete Dams (SSHM4Dams) - PTDC/ECI-EGC/5332/2020.

## REFERENCES

[1] Farinha, M.L.B., Lemos, J.; Maranha das Neves, E. (2012). Analysis of foundation sliding of an arch dam considering the hydromechanical behaviour, Frontiers of Structural Civil Engineering, vol. 6(1), pp 35–43

[2] Farinha, M.L.B., Lemos, J.; Maranha das Neves, E. (2012). Modelação tridimensional das pressões da água na fundação da barragem de Alqueva. Proceedings do 13º Congresso Nacional de Geotecnia, LNEC, Lisboa.

[3] Farinha, M.L.B., Monteiro Azevedo, N., Schclar Leitão, N.; Rocha de Almeida, J.; Oliveira, S. (2022). Sliding Stability Assessment of Concrete Dams Using a 3D Discontinuum Hydromechanical Model Following a Discrete Crack Approach. Geotechnics 2022, 2, pp 133-157.

[4] Monteiro Azevedo, N.; Farinha, L. (2015). Um modelo hidromecânico para a análise de fundações de barragens gravidade em betão, Geotecnia, 2015, 133, pp 5-33 (in Portuguese).

[5] Belytschko, T. e O' Neal, M. (1991). Contact-impact by the pinball algorithm with penalty and lagrangian methods, International Journal for Numerical Methods in Engineering, vol. 31(3), pp 547–572.

[6] Ahn, T. Y., Ryu, S., Song, J. J. & Lee, C, (2009). A New Contact Method using Inscribed Sphere for 3D Discontinuous Deformation Analysis. Analysis of Discontinuous Deformation: New Developments and Applications. 127-134.

[7] Ahn, T. Y., Song, J. J. (2012). New Contact Resolution Algorithm using Two-stage Contact Definition and Rounding Scheme in 3D DDA. In Proceedings of the 10th International Conference on Analysis of Discontinuous Deformation, Advances in Discontinuous Numerical Methods and Applications in Geomechanics and Geoengineering Editors. pages 101-106.

[8] Farinha, M.L B., Monteiro Azevedo, N., Candeias, M. (2017). Small Displacement Coupled Analysis of Concrete Gravity Dam Foundations: Static and Dynamic Conditions, Rock mechanics & Rock Engineering, , Vol 50 (2), pp 439-464.

[9] Monteiro Azevedo, N.; Lemos, J. (2022). A Hybrid Particle/Finite Element Model with Surface Roughness for Stone Masonry Analysis. Applied Mechanics, 3, pp 608–627.

[10] Ivars, D., Pierce, M., Darcel, C., Montes, J., Potyondy, D., Young, R. e Cundall, P. (2011). The synthetic rock mass approach for jointed rock mass modelling, International Journal of Rock Mechanics & Mining Sciences, vol. 48 (2), pp 219-244.

[11] Scholtes, L. e Donzé, F. (2012). Modelling progressive failure in fractured rock masses using a 3D discrete element method, International Journal of Rock Mechanics & Mining Sciences, vol. 52, pp 18-30.

[12] Pulatsu, B., Erdogmus, E., Lourenço, P.B. et al. (2021). Numerical modeling of the tension stiffening in reinforced concrete members via discontinuum models. Comp. Part. Mech. 8, 423–436. https://doi.org/10.1007/s40571-020-00342-5

[13] Ghazvinian, E.; Diederichs, M.; Quey, R. (2014). 3D Random Voronoi grain-based models for simulation of brittle rock damage and fabric-guided micro-fracturing. J. Rock Mech. Geotech. Eng., 6, 506–521.

[14] Azevedo, N. (2003). A rigid particle discrete element model for the fracture analysis of plane and reinforced concrete. PhD Thesis, Heriot-Watt University, Scotland

[15] Lemos, J. (1995). Metodologias para deteção e atualização de contactos em modelos de elementos discretos. Proceedings do IV Encontro Nacional de Mecânica Computacional, Lisboa, pp. 61-72 (in Portuguese).

[16] Goodman, R. e Taylor, R.; Brekke, T. (1968). A model for the mechanics of jointed rock, Journal of the Soil Mechanics and Foundations Division (ASCE), vol. 94(SM3), pp 637-659.

[17] Hohberg, J. (1992). A joint element for the nonlinear dynamic analysis of arch dams. PhD Thesis. Institute of Structural Engineering, ETH, Zurich, Switzerland.

[18] Itasca (2013). 3DEC - 3-Dimensional Distinct Element Code, Version 5.0, User's Manual. Itasca Consulting Group, Minneapolis, USA.